

Payman Rezaee\* and Michael Höft

# Design and Fabrication of a Novel Compact Bandpass Filter to Improve Spurious-Free Band

DOI 10.1515/freq-2016-0210

Received July 6, 2016

**Abstract:** In this paper, a new microstrip slow wave open loop resonator is proposed. This resonator overcomes the substantial limitation of the conventional slow wave open loop resonators, which limits the spurious-free band of those resonators. The new proposed resonator improves the spurious-free band up to 8 times of the fundamental frequency, which is 3.16 times of the conventional slow wave open loop resonators. For the proposed resonator the coupling factor and the external quality factor curves, which are the design curves of a narrowband filter, are extracted using a full wave simulator, i. e. HFSS. These curves are utilized for the design of two three-pole Chebyshev bandpass filters. One of these filters is fabricated. Simulation and measurement results are reported which are in good agreement. Designed filters provide 75% and 83% of footprint reduction in comparison with the conventional open loop resonator filters. Different parameters which can improve the spurious-free band are explained in the paper.

**Keywords:** bandpass filter, compact filter, microstrip filter, slow wave resonator

## 1 Introduction

In wireless communication systems, small size, low cost, and high performance filters are highly desired. Microstrip filters, which provide planar structure, simple fabrication process, and integration possibility with planar circuits of a microwave system, are among the best choices. In recent years enormous efforts have been carried out to fulfill the required size and

performance of microwave filters based on the microstrip technology [1]–[15].

In [2], a half wavelength transmission line resonator with a pair of tap-connected open-ended stubs and in [3], a quarter wavelength microstrip resonator was utilized to design compact bandpass filters. The first spurious response ( $f_1$ ) of an ideal half wavelength resonator occurs at  $2 \times f_0$ , where  $f_0$  is the fundamental resonant frequency, and in the case of quarter wavelength it occurs at  $3 \times f_0$ . Better spurious response of quarter wavelength resonators is at the expense of shorted vias, which connect the end of each resonator to the ground. Folded quarter wavelength resonator is another choice to make the filter area smaller but again the first spurious occurs at  $3 \times f_0$  [4]. In order to avoid the shorted vias and make the filter size compact, one can use hairpin resonators in which  $f_1 = 2 \times f_0$  because the resonator is half wavelength long. In [5], a step impedance hairpin resonator was introduced with a two-layer substrate for a compact filter design. This filter was composed of four stepped-impedance hairpin resonators located on two stacked microstrip layers, and the couplings between the resonators on the upper layer and those on the lower one was obtained by using three coupling apertures etched on a common ground plane placed between the two layers. Although it improves the first spurious response to approximately  $2.46 \times f_0$  and provides a wider spurious-free band in comparison with a conventional hairpin, however the spurious performance is still worse than a quarter wavelength resonator. The same spurious performance is reported in [6] for a hexagonal stepped impedance resonator. The spurious response of the hairpin resonator was further improved in [7] to  $f_1 = 2.85 \times f_0$  by taking advantage of a new interdigital hairpin resonator. The same spurious performance can be seen for a new interdigital resonator reported in [8]. Although a lot of efforts have been carried out to reduce the microstrip filter size using dual-mode resonators [9], concentric open loop resonators [10], spiral open loop resonators [11], composite left/right handed quarter wave resonators [12], and twisted modified asymmetric split ring resonators [13], however none of these structures provide a better spurious response than a quarter wavelength resonator. Even in the case of dual-mode resonator [9] and twisted modified

\*Corresponding author: Payman Rezaee, Chair of Microwave Engineering, Technical Faculty, Institute of Electrical and Information Engineering, Christian-Albrechts-University of Kiel, Kiel, Germany, E-mail: Payman.Rezaee@tf.uni-kiel.de

Michael Höft, Chair of Microwave Engineering, Technical Faculty, Institute of Electrical and Information Engineering, Christian-Albrechts-University of Kiel, Kiel, Germany, E-mail: Michael.Hoef@tf.uni-kiel.de

asymmetric split ring resonator [13], the spurious-free band is smaller than  $2 \times f_0$ . A successful approach to improve the spurious performance of a microstrip filter is based on the slow wave concept introduced in [14]. In this paper, based on an end-coupled slow wave resonator, the first spurious response occurs at  $3.6 \times f_0$ . This resonator can only be implemented in few filtering configurations. Ref [15] solved the problem by introducing another slow wave open loop resonator at the price of narrower spurious-free band ( $f_1 = 2.9 \times f_0$ ).

In this paper, the substantial limitation of the conventional slow wave open loop resonator [15] for a wider spurious-free band is resolved. In Section 2, functionality and limitation of the conventional slow wave open loop resonator is understood using simulation results of HFSS. In Section 3, the geometry of the new slow wave resonator is proposed and the spurious-free region is compared with the conventional one. Section 4 is devoted to filter design and reporting the simulation and measured results and finally Section 5 concludes the paper.

## 2 Conventional slow wave open loop resonator

When a transmission line resonator is loaded by two capacitors at both ends, the resonant frequency of the new structure is shifted down, which indicates the slow wave effect. Another behavior in this regard is that the ratio of the first spurious to the fundamental frequency is increased. In Ref. [14], based on the equivalent circuit of a slow wave resonator which is composed of a transmission line with two capacitors at both ends, the eigenequation for the fundamental resonant frequency was derived and the above mentioned behavior was concluded. In Ref. [15], corresponding formulae have been extracted by writing the ABCD parameters of a transmission line

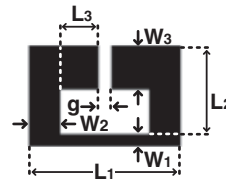


Figure 1: A typical slow-wave open loop resonator.

resonator which has been loaded by two capacitors at both ends and is satisfying the boundary conditions. Inspiring this idea, the slow wave open loop resonator was introduced in [15]. Figure 1 demonstrates a typical slow wave open loop resonator. As is seen, it is composed of a microstrip transmission line with both ends loaded with folded stubs. If the capacitance of the folded stubs is increased by an increase of the folded line widths ( $W_2$  and  $W_3$  of Figure 1), the fundamental resonant frequency decreases and the spurious-free band of the resonator response increases. As an example, the fundamental and the first spurious resonant frequencies for the structure of Figure 1 and also their ratio have been plotted versus  $L_3$  in the range of  $[0, 2.75 \text{ mm}]$  in Figure 2. Results have been calculated using the eigenmode solver of HFSS. The structure of the resonator has been realized on a substrate with thickness and relative permittivity equal to 1.27 mm and 9.2, respectively. Other physical parameters of the structure for this simulation have been set as follows:  $L_1 = 8$ ,  $W_1 = 1$ ,  $L_2 = 5$ ,  $W_2 = 1$ , and  $W_3 = 4$  (all in mm). As is seen, increasing  $L_3$  adds more capacitance to both ends, thus contributing to the slow-wave effect, and the fundamental resonant frequency decreases (from 3.42 GHz for  $L_3 = 0$  to 2.75 GHz for  $L_3 = 2.75 \text{ mm}$ ). Over the whole variation range of  $L_3$ , the ratio of the first spurious and the fundamental frequency changes from 1.93 to 2.53. As can be concluded, the second harmonic has been suppressed by the use of this resonator. Therefore it can be utilized for filter design if suppressing the second harmonic is required.

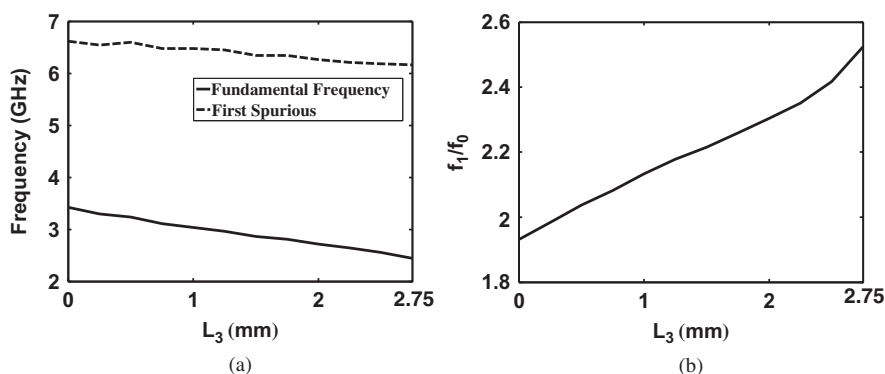


Figure 2: (a) Fundamental and first spurious frequency response and (b) their ratio versus  $L_3$  for the structure of Figure 1.

Considering Figure 2(b), it is impossible to suppress the third harmonic with the resonator of Figure 1. In order to overcome this problem, larger values of loading are required which is not possible through the use of wider lines because of the physical limitations. In other words, by increasing  $L_3$  and  $W_3$  or  $W_2$  for a higher capacitive loading, the gap between two arms ( $g$ ) will be closed and the slow wave resonator will be converted to a patch resonator. Therefore, the nature of the resonator is changed. In Section 3, a new slow-wave open loop resonator which will solve the problem of the conventional one is proposed.

### 3 Proposed slow wave resonator and its behavior

As was mentioned in Section 2, increasing the value of the capacitance at both ends of the resonator generates a stronger slow-wave effect. It can produce a wider spurious-free region. In order to increase the capacitance of the folded stubs, the use of some metalized cylinders at these folded sides is proposed. The metalized cylinders increase the value of capacitance because the effective distance between the folded stubs and the ground plane decreases. Figures 3(a)–(c) present the proposed slow-

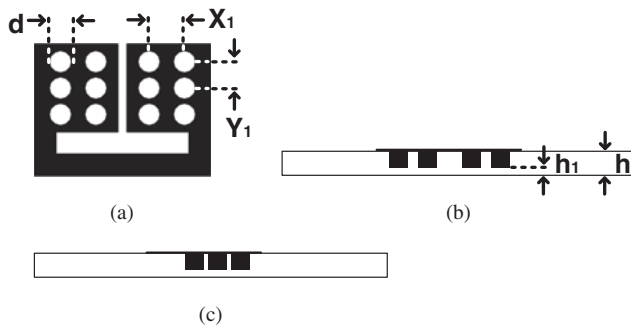


Figure 3: Proposed slow-wave open loop resonator; (a) top view, (b) front view, and (c) side view.

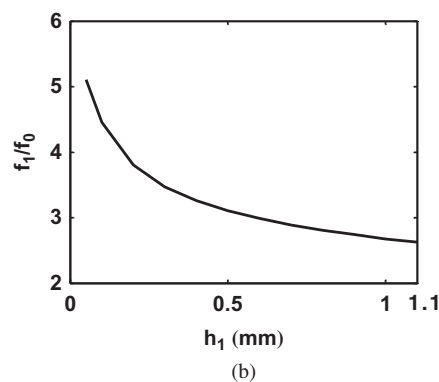
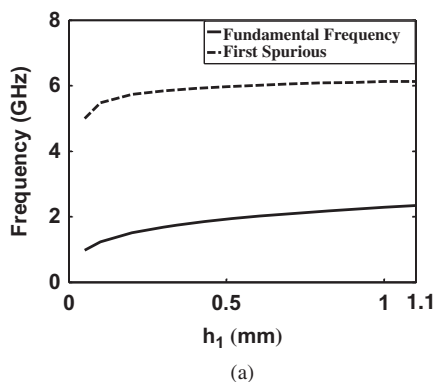


Figure 4: (a) Fundamental and first spurious frequency response and (b) their ratio, versus  $h_1$  for the proposed structure (Figure 3).

wave resonator from top, front, and side view, respectively. According to this figure, a smaller  $h_1$  can produce a larger slow-wave effect. In order to fabricate the proposed resonator, one can drill the required cylinders inside the substrate with the required diameter and depth ( $d$  and  $h-h_1$ , respectively) using standard drilling machine. The drilled cylinders will then be filled by inserting metallic rods. If each metallic rod has a hollow in center, one can fill the inserted hollow metallic rods with soldering material. As another option for the fabrication process of the proposed resonator, one can use laser beam instead of drilling machine.

In order to prove the potential of the proposed resonator for the improvement of the spurious-free region, the curves of  $f_0$ ,  $f_1$ , and  $f_1/f_0$ , in which  $f_0$  and  $f_1$  are the fundamental and the first spurious frequency, respectively, are extracted for the proposed structure (Figure 3) versus  $h_1$ . The results are demonstrated in Figure 4. The dimensions of the resonator were selected as in Section 2 and read as follow:  $L_1=8$  mm,  $W_1=1$  mm,  $L_2=5$  mm,  $W_2=1$  mm,  $L_3=2.8$  mm, and  $W_3=4$  mm. The same substrate was used with permittivity and thickness equal to 9.2 and 1.27 mm, respectively. The dimensions of the metalized holes and the spacing between their centers in  $x$ - and  $y$ -direction have been selected to be equal to  $d=1$  mm,  $X_1=1.6$  mm, and  $Y_1=1.2$  mm, respectively (see Figure 3). The variation range of  $h_1$  is equal to  $[0.05$  mm, 1.1 mm]. Table 1 presents the maximum and the minimum values of the fundamental frequency and the ratio of  $f_1$  to  $f_0$  for these values, according to Figure 4.

Comparing the results of Table 1 with the results of Section 2 shows that the proposed slow-wave resonator is able to improve the spurious-free region by more than two times compared to the conventional slow wave resonator up to  $5.11 \times f_0$  and is also able to decrease the fundamental frequency to 0.3564 times of that of the conventional slow wave resonator with the same dimensions.

Figure 5(a) shows the effect of diameter of the metalized cylinders (the variation range is between  $[0.6$  mm to

**Table 1:** Fundamental frequency and the ratio of the first spurious to the fundamental frequency at the beginning and at the end of the variation range of  $h_1$ , according to Figure 4.

$h_1$ (mm)	$f_0$ (GHz)	$f_1/f_0$
0.05	0.98	5.11
1.1	2.34	2.63

1.2 mm]) on the fundamental and the first spurious resonant frequencies for a specific value of  $h_1$  ( $h_1 = 0.05$  mm). Other physical dimensions and the substrate properties are the same as Figure 3. Figure 5(b) presents the ratio of  $f_1$  to  $f_0$ . As is seen, by increasing the diameter, the slow wave effect increases, i.e. the fundamental resonant frequency decreases and the ratio of  $f_1$  to  $f_0$  increases. Table 2 presents the maximum and the minimum values of the fundamental frequency and the ratio of  $f_1$  to  $f_0$  for  $d = 0.6$  mm and 1.2 mm, according to Figure 5. Comparing the first row of Table 1 ( $h_1 = 0.05$  mm) and the second row of Table 2 ( $d = 1.2$  mm) shows that by increasing  $d$  from 1 mm to 1.2 mm,  $f_1/f_0$  improves from 5.1 to 6.05 and the fundamental frequency decreases from 0.98 GHz to 0.877 GHz which means more miniaturization possibility.

As was mentioned in the previous paragraphs, by increasing the diameter of the metalized cylinders or increasing their heights (decreasing  $h_1$ ), the spurious-free band improves. Another approach to generate a wider spurious-free band is to increase the number of metalized cylinders per each resonator. Figure 6 shows a resonator with three columns of metalized cylinders per each side.  $X_1$  and  $Y_1$  are both selected to be equal to 1.2 mm,  $d = 1$  mm and  $h_1 = 0.05$  mm. Other dimensions are the same as Figure 3 and read as follow:  $L_1 = 8$  mm,  $W_1 = 1$  mm,  $L_2 = 5$  mm,  $W_2 = 1$  mm,  $L_3 = 2.8$  mm, and  $W_3 = 4$  mm. The same substrate was used with permittivity and thickness equal to 9.2 and 1.27 mm, respectively. For this case,  $f_0$  is equal to 0.852 GHz and  $f_1/f_0$  is equal to 5.9. Comparing the results with the first row of Table 1 ( $h_1 = 0.05$  mm) shows the positive effect of adding extra rods to the proposed slow wave resonator (see Figures 3 and 6) on the resonator behavior,

**Table 2:** Fundamental frequency and the ratio of the first spurious to the fundamental frequency at the beginning and at the end of the variation range of  $d$ , according to Figure 5.

$d$ (mm)	$f_0$ (GHz)	$f_1/f_0$
0.6	1.277	3.86
1.2	0.877	6.05

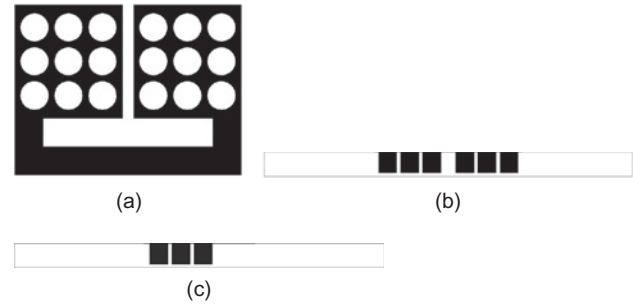


**Figure 6:** Proposed slow-wave open loop resonator with 3 × 3 metallic cylinders for each side; (a) top view, (b) front view, and (c) side view.

i.e. improving the spurious-free band and decreasing the resonant frequency of the fundamental mode. For the above mentioned dimensions, the effect of metallic rod diameters on the resonant frequency and the spurious behavior in the range of  $d = [0.6$  mm to 1.2 mm] has been extracted using HFSS (see Figure 7). The results are summarized in Table 3 for two values of  $d$  ( $d = 0.6$  mm and  $d = 1.2$  mm). As is seen  $f_1/f_0$  is improved to 8 and  $f_0$  is decreased to 0.766 GHz. In the next section, the proposed resonator is utilized for filter design.

## 4 Filter design based on the proposed resonator

In the following, two three-pole bandpass Chebyshev filters are designed based on the proposed slow-wave resonator (Figure 3). Table 4 presents the required filter

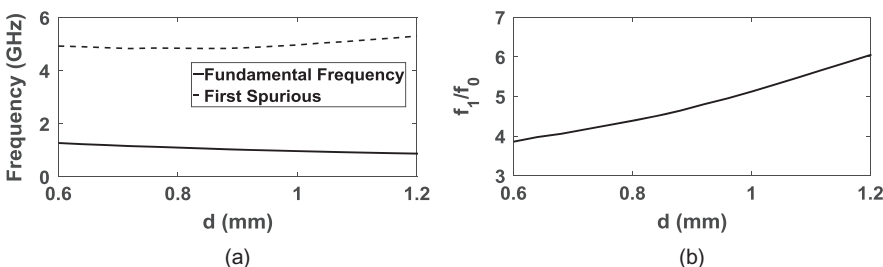


**Figure 5:** (a) Fundamental and first spurious frequency response and (b) their ratio, versus  $d$  for the proposed structure (Figure 3). The value of  $h_1$  is equal to 0.05 mm.

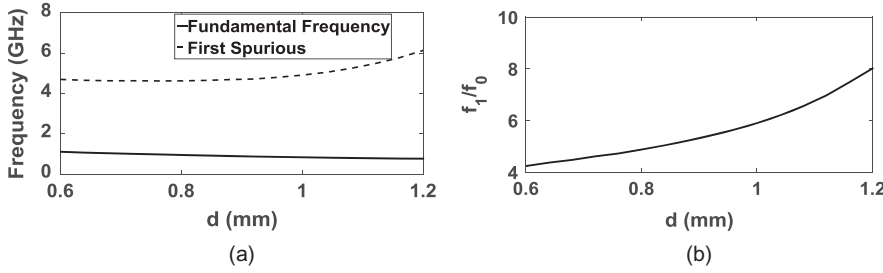


**Figure 7:** (a) Fundamental and first spurious frequency response and (b) their ratio, versus  $d$  for the proposed structure of Figure 6. The value of  $h_1$  is equal to 0.05 mm.

**Table 3:** Fundamental frequency and the ratio of the first spurious to the fundamental frequency at the beginning and at the end of the variation range of  $d$ , according to Figure 7.

$d$ (mm)	$f_0$ (GHz)	$f_1/f_0$
0.6	1.110	4.24
1.2	0.766	8.02

**Table 4:** Required specifications of filter 1 and 2.

	N	$f_0$ (GHz)	FBW (%)	$R_L$ (dB)	Type
Filter 1	3	1.641	4.6	20	Chebyshev
Filter 2	3	1.240	3.4	20	Chebyshev

specifications, where  $N$ ,  $f_0$ , FBW, and  $R_L$  are order of the filter, center frequency, fractional bandwidth, and return loss, respectively. As is seen, the required fractional bandwidth and center frequency of filter 1 is equal to 4.6% and 1.641 GHz, and of filter 2 to 3.4% and 1.24 GHz, respectively.

The dimensions of the utilized resonator are as follows:  $L_1 = 8$ ,  $W_1 = 1$ ,  $L_2 = 5$ ,  $W_2 = 1$ ,  $L_3 = 2.8$ ,  $W_3 = 4$ ,  $d = 1$ ,  $X_1 = 1.6$ , and  $Y_1 = 1.2$  (all in mm). The resonator was realized on a substrate with permittivity and thickness equal to 9.2 and 1.27 mm, respectively. For filters 1 and 2, the value of  $h_1$  was selected to be equal to 0.27 mm and 0.1 mm, respectively, in order to realize the desired center frequencies.

For the above mentioned specifications, the coupling factors and the external quality factor ( $Q_e$ ) are calculated using (1) [16]. Calculated values for filters 1 and 2 are given by (2) and (3), respectively.

$$Q_e = \frac{g_0 g_1}{\text{FBW}} \quad (1)$$

$$m_{12} = m_{23} = \frac{\text{FBW}}{\sqrt{g_1 g_2}}$$

$$M_1 = \begin{bmatrix} 0 & 0.0474 & 0 \\ 0.0474 & 0 & 0.0474 \\ 0 & 0.0474 & 0 \end{bmatrix}, \quad Q_e = 18.5 \quad (2)$$

$$M_2 = \begin{bmatrix} 0 & 0.035 & 0 \\ 0.035 & 0 & 0.035 \\ 0 & 0.035 & 0 \end{bmatrix}, \quad Q_e = 25.1 \quad (3)$$

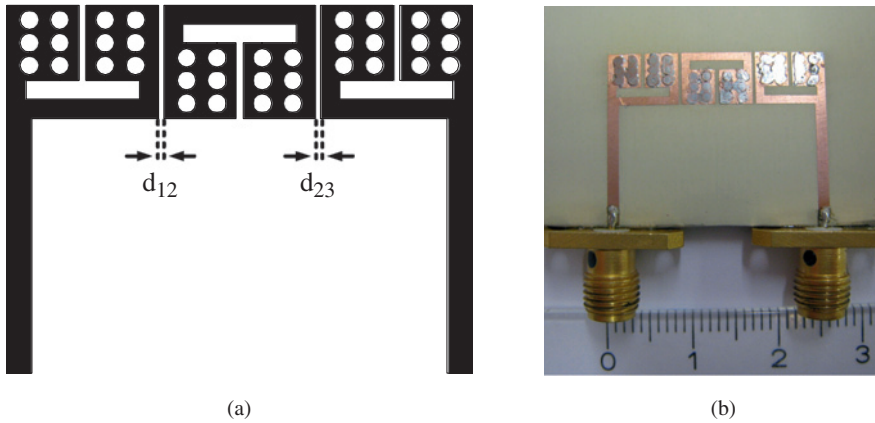
where  $g_1$  and  $g_2$  are the normalized equivalent circuit elements of the lowpass prototype and  $g_0$  is the normalized source impedance.

Figure 8(a) demonstrates the layout of filters 1 and 2. The required spacing between the resonators is extracted using the conventional full-wave approach which was explained in [16]. In this approach, two resonators are coupled to each other when they are decoupled from the remainder and according to the following equation the value of coupling is calculated.

$$m_{ij} = \frac{f_{p2}^2 - f_{p1}^2}{f_{p2}^2 + f_{p1}^2} \quad (4)$$

where  $f_{p1}$  and  $f_{p2}$  are the lower and the higher resonant frequencies by placing short circuit and open circuit at the symmetry plane of the coupled resonators. Figure 9 shows the variation of the coupling factor versus the distance between the coupled resonators for filter 1, which has been calculated using HFSS. In the inset of this figure, the geometry of the coupled resonators has been demonstrated. The same curve is extracted for filter 2 while  $h_1$  is set to 0.1 mm (This curve has not been shown here because of the similarity). Based on the extracted coupling factor curves,  $d_{12} = d_{23} = 0.3$  mm for filter 1 and  $d_{12} = d_{23} = 0.15$  mm for filter 2. For the realization of the required external quality factor a tapped line feed probe is used (see the inset of Figure 10). There are three parameters which affect the value of external quality factor, i.e. the length ( $L_f$ ), the width ( $W_f$ ), and the position of the feed probe ( $d_f$ ). Figure 10 shows the external quality factor curve versus  $L_f$  while  $W_f$  and  $d_f$  are set to 1.5 mm and 0, respectively, for filter 1. The same curve can be calculated for filter 2 (it has not been shown here). The external quality factor curve is calculated using the following equation.

$$Q_{\text{ext}} = \frac{\omega_0}{\Delta\omega_{\pm 90^\circ}} \quad (5)$$



**Figure 8:** (a) Layout and (b) physical structure of the fabricated filter using the proposed slow-wave open loop resonator of Figure 3.

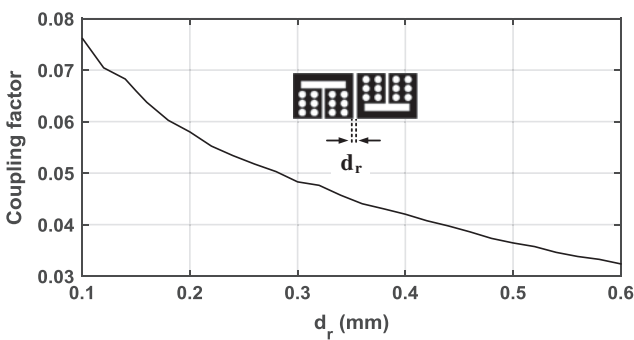


**Figure 9:** Coupling factor of the coupled resonators versus the distance between them for filter 1 (coupled resonators are shown in inset).

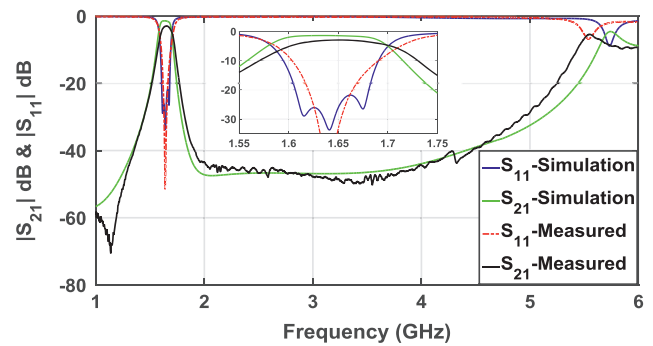


**Figure 11:** Measured and simulated response of the fabricated filter (filter 1) using the proposed slow-wave open loop resonator of Figure 3 (in-band response is shown in inset).

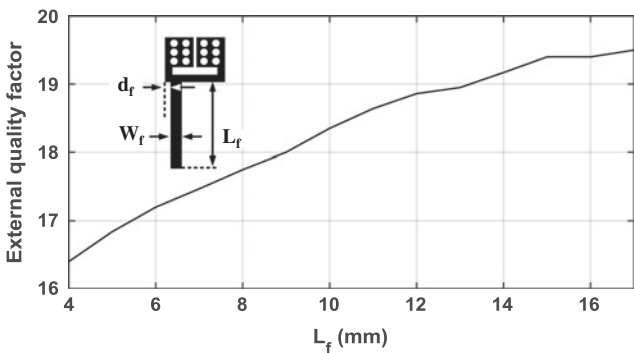


**Figure 10:** External quality factor curve for filter 1 versus  $L_f$ .  $W_f$  and  $d_f$  have been selected to be equal to 1.5 mm and 0, respectively (the resonator including the feed probe is shown in inset).

where  $\omega_0$  is the resonant frequency of the resonator including feed probe and  $\Delta\omega_{\pm 90^\circ}$  are the frequencies in which the phase of  $S_{11}$  is changed by  $+90^\circ$  and  $-90^\circ$ , respectively [16]. Based on the design curve of Figure 10, the required length of the feed probe for filter 1 is extracted, i.e.  $L_f=11.5$  mm. For filter 2 it is equal to  $L_f=13.5$  mm, while  $W_f=1.3$  mm and  $d_f=0.3$  mm.

The physical structure of the fabricated filter (filter 1) and its measured response accompanied with the full-wave one are displayed in Figures 8(b) and 11, respectively. The simulation result of filter 2 using a full-wave simulator (HFSS) is depicted in Figure 12. According to Figures 11 and 12, the ratio of the center frequency of filters 1 and 2 to the first spurious frequency will be 3.48 and 4.28, respectively. This clearly shows the improved spurious-free band of the proposed resonator. This region can be

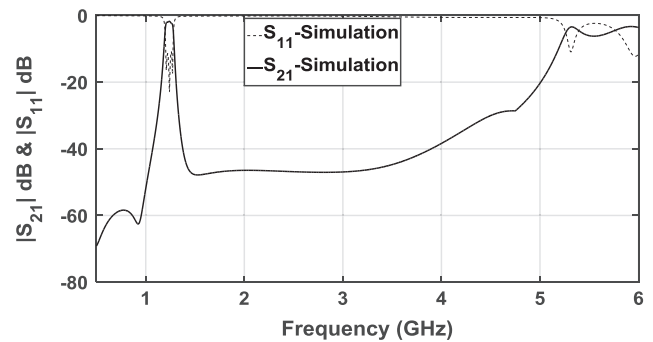


**Figure 12:** Full-wave simulation results of filter 2.

even wider for smaller values of  $h_1$  (see Table 1), larger diameter of the metallic rods (see Table 2) or by increasing the number of metallic rods (see Figure 6 and Table 3). The value of insertion loss of the fabricated filter and the simulated version at center frequency is 3 dB, and 1.4 dB, respectively, which present an unloaded quality factor of 90 and 160, respectively, for the fabricated filter and its simulation model. In the simulation model, strips and metallic cylinders are supposed to be copper, which are fabricated on a substrate with dielectric loss tangent of 0.0022. The difference between the insertion loss of the simulation and measurement results can be the effect of feed ports, roughness of the surface after soldering the metallic cylinders, and the fabrication tolerances of the metalized cylinders.

Another important feature of the proposed resonator is its potential for miniaturization. In order to demonstrate this possibility, a conventional square open loop resonator was designed to have the same resonant frequency as is produced by the proposed resonator. If the resonator of filter 2 is replaced by a 14 mm × 14 mm square open loop resonator on the same substrate with the same gap size and width ( $W=1$  mm), the same resonant frequency is generated. If the resonator of filter 2 is replaced by the new one which has  $h_1$  equal to 0.05 mm, the dimensions of a square open loop resonator (SOLR) will be 17 mm × 17 mm in order to generate the same frequency. The dimensions of the proposed resonator are 8 mm × 6 mm in both cases (case 1 with  $h_1=0.1$  mm and case 2 with  $h_1=0.05$  mm). Therefore in case 1, the area of the proposed resonator is by more than 75% and in case 2 by more than 83% reduced in comparison with a conventional SOLR on the same substrate. For case 1 and case 2, the dimensions of the proposed resonator are about  $(0.1091 \lambda_{g0}) \times (0.0818 \lambda_{g0})$  and  $(0.0823 \lambda_{g0}) \times (0.0617 \lambda_{g0})$ , respectively, where  $\lambda_{g0}$  is the guided wavelength of a 50  $\Omega$  line on the substrate at the resonant frequency. According to Tables 2 and 3, further miniaturization can be achieved by increasing the diameter of the metallic cylinders or increasing their numbers.

## 5 Conclusions

In this paper, a new compact microstrip slow wave open loop resonator was proposed. This resonator improved the spurious-free band of the conventional slow wave open loop resonator by factor of more than 3 up to 8 times of the fundamental frequency. This resonator can also drastically decrease the footprint of a

conventional open loop resonator. Different mechanisms for improving the spurious response of the resonator was explained. Based on the proposed resonator two filters were designed and one of them was fabricated. Design curves have been calculated using HFSS. Simulation and measurement results were reported which are in good agreement.

## References

- [1] P. Rezaee and M. Höft, "A new compact microstrip slow wave open loop resonator filter with improved spurious-free band," in *Proc. German Microwave Conf.*, Bochum, Germany, 14–16 March, 2016, pp. 217–220.
- [2] L. Zhu and W. Menzel, "Compact microstrip bandpass filter with two transmission zeros using a stub-tapped half-wavelength line resonator," *IEEE Microw. Wirel. Compon. Lett.*, vol. 13, no. 1, pp. 16–18, Jan. 2003.
- [3] J. R. Lee, J. H. Cho, and S. W. Yun, "New compact bandpass filter using microstrip  $\lambda/4$  resonators with open stub inverter," *IEEE Microw. Guided Wave Lett.*, vol. 10, no. 12, pp. 526–527, Dec. 2000.
- [4] P. H. Deng, Y. S. Lin, C. H. Wang, and C. H. Chen, "Compact microstrip bandpass filters with good selectivity and stopband rejection," *IEEE Trans. Microw. Theory Tech.*, vol. 54, no. 2, pp. 533–539, Feb. 2006.
- [5] A. Djaiz and T. A. Denidni, "A new compact microstrip two-layer bandpass filter using aperture-coupled SIR-hairpin resonators with transmission zeros," *IEEE Trans. Microw. Theory Tech.*, vol. 54, no. 5, pp. 1929–1936, May 2006.
- [6] R. J. Mao, X. H. Tang, L. Wang, and G. H. Du, "Miniaturized hexagonal stepped-impedance resonators and their applications to filters," *IEEE Trans. Microw. Theory Tech.*, vol. 56, no. 2, pp. 440–448, Feb. 2008.
- [7] J. Zhu and Z. Feng, "Microstrip interdigital hairpin resonator with an optimal physical length," *IEEE Microw. Compon. Lett.*, vol. 16, no. 12, pp. 672–674, Dec. 2006.
- [8] T. Yang, M. Tamura, and T. Itoh, "Compact hybrid resonator with series and shunt resonances used in miniaturized filters and balun filters," *IEEE Trans. Microw. Theory Tech.*, vol. 58, no. 2, pp. 390–402, Feb. 2010.
- [9] J. S. Hong and S. Li, "Theory and experiment of dual-mode microstrip triangular patch resonators and filters," *IEEE Trans. Microwave Theory Tech.*, vol. 52, no. 4, pp. 1237–1243, April 2004.
- [10] L. Athukorala and D. Budimir, "Compact filter configurations using concentric microstrip open-loop resonators," *IEEE Microw. Wireless Compon. Lett.*, vol. 22, no. 5, pp. 245–247, May 2012.
- [11] P. Rezaee, M. Tayarani, and R. Knöchel, "Miniaturized microstrip filter design using active learning method," *Radioengineering*, vol. 20, no. 4, pp. 857–865, Dec. 2011.
- [12] T. Yang, P. L. Chi, and T. Itoh, "Compact quarter-wave resonator and its applications to miniaturized diplexer and triplexer," *IEEE Trans. Microw. Theory Tech.*, vol. 59, no. 2, pp. 260–269, Feb. 2011.

- [13] J. Li, Y. Huang, G. Wen, X. Xue, and J. Song, "Compact and high-selectivity microstrip bandpass filter using two-stage twist-modified asymmetric split-ring resonators," *Electron. Lett.*, vol. 51, no. 8, pp. 635–637, Apr. 2015.
- [14] J. S. Hong and M. J. Lancaster, "End-coupled microstrip slow-wave resonator filter," *Electron. Lett.*, vol. 32, no. 16, pp. 1494–1496, Aug. 1996.
- [15] J. S. Hong and M. J. Lancaster, "Theory and experiment of novel microstrip slow-wave open-loop resonator filters," *IEEE Trans. Microw. Theory Tech.*, vol. 45, no. 12, pp. 2358–2365, Dec. 1997.
- [16] J. S. Hong and M. J. Lancaster, *Microstrip Filters for RF/Microwave Applications*. New York: John Wiley & Sons, 2001.